The Role of Rheological Properties in Mucociliary Transport by Frog Palate Ciliated Model

Danny M. Yu,[1] Gordon L. Amidon,[1,3] Norman D. Weiner,[1] David Fleisher,[1] and Arthur H. Goldberg[2]

Received June 1, 1994; accepted July 15, 1994

The effect of viscoelastic properties on mucociliary transport rate was investigated using the frog palate ciliated model. Mucociliary transportability of several hydrophilic polymeric gels with widely different viscoelastic characteristics were tested on the frog palate mucociliary model. An apparent negative relationship is observed between the relative transport rate (*TR*) and storage (G_1) or loss (G_2) modulus. However, a minimum in relative transport rate is observed at an apparent loss tangent (tan δ) value of between 0.7 and 0.9. A theoretical model for mucociliary transport is presented. The model predicted a minimum in transport rate at tan δ equal to 1.74 after adjustment for primary variation due to storage modulus (G_1), which is in agreement with the observed frog palate transport rate. The model isolates the loss tangent (tan δ) and the magnitude of the complex modulus ($|G^*|$) as the important viscoelastic parameters for mucociliary transport. Optimum rheological characteristics with respect to slow transport rate can be achieved by using hydrophilic polymer gels with a large complex modulus and simultaneously with a loss tangent equal to 1.74.

KEY WORDS: viscoelastic property; mucociliary transport; frog palate; theoretical modeling of mucociliary transport.

INTRODUCTION

Although the oral route of drug administration is considered to be the most convenient means of introducing drugs into systemic circulation, there are some limitations such as when extensive first-pass elimination or degradation by acid or enzymes in the GI system occur or when the drug is poorly absorbed by the intestinal wall. This is especially true for peptide drugs in which absorption via the GI tract are not expected to be sufficient enough to display a useful therapeutic effect. Therefore, the major route of administration of these bioactive peptide drugs so far has been by parenteral injection. However, the inconvenience and invasive nature of this route of administration has led to the investigation for an alternate route of delivery for these drugs. Recently, the nasal route is considered a viable alternative mode of drug administration. The advantage include low enzyme activity in the nasal mucosa compared to the GI tract, elimination of first-pass hepatic metabolism, a rich vascularity and large surface area available for rapid absorption into the systemic circulation and ease of administration (1,2,3).

In spite of all the advantages cited above, the rapid clearance of a drug from the nasal cavity by the mucociliary clearance system will influence the extent of absorption and bioavailability of a drug administered intranasally. The mucociliary system represents the principal mechanism of defense in the respiratory tract by elimination of foreign bodies from the surface of the air-exposed epithelium. The epithelium is covered by a two-layer system: a bottom low viscosity periciliary layer approximately as deep as the length of the cilia, and on the surface a viscoelastic mucus layer (4). The cilia beat constantly and in synchronization at a frequency in the range of 10–20 Hz (5,6) in the low viscosity periciliary layer, and transport occurs via interaction of the cilia tip with the mucus blanket (7). Therefore, intranasal mucociliary clearance is a composite activity that depends on the magnitude of, and synchronized beating of the cilia as well as the viscoelastic properties of the overlying mucus layer (8). The rate of flow depends on the complex interaction between the dynamics, i.e., the mechanism by which energy is imparted to the fluid and lost by the fluid and the rheology of the fluid, i.e., the specific properties of the fluid relating to flow and deformation (9). In this respect, the rheological properties are major determinants of mucociliary clearance. The normal nasal transit time has been reported to be 12 to 15 minutes (10). This relatively short time for absorption to take place in the nasal cavity is a major limitation particularly for slowly absorbed compounds like peptides and proteins.

Recently, a viscoelastic mucoadhesive polymeric gelling system was used to optimize nasal formulation characteristics in an attempt to maintain the drug in contact with the nasal mucosal membrane for a longer time (11). Several theoretical models have been developed for mucociliary transport (12,13). However, in spite of the sophistication and complexity of the mathematics involved in the development of the theoretical models, many of the features found in the actual mucociliary transport system, especially the viscoelastic nature of the mucus layer, were not adequately reflected in the models and the inter-relationship between the viscoelastic properties of polymer gel and mucociliary transport rate have not been established. Therefore, the present study is undertaken to delineate the role of viscoelastic characteristics on mucociliary transport. Toward this objective, this paper will focus on i) development of an *in vitro* (or *ex vivo*) model using excised frog palate for measuring mucociliary transport rate of polymers encompassing a range of viscoelastic properties; ii) investigating the relationship between viscoelastic characteristics and mucociliary transport rate; and iii) development of a relevant mathematical model to describe and correlate mucociliary transport rate with rheological parameters.

THEORETICAL MODEL DEVELOPMENT

Model Analysis Outline

The model for mucociliary flow is schematically represented by a one dimensional flow problem illustrated in fig-

[1] College of Pharmacy, University of Michigan, Ann Arbor, Michigan 48109-1065.
[2] Rugby-Darby Group Companies, Inc., Rockville Center, New York 11570.
[3] To whom correspondence should be addressed.

0724-8741/94/1200-1785$07.00/0

ure 1. Stress generated by cilia is transmitted through the viscoelastic mucus layer to the underside of the viscoelastic polymer layer. The normal thickness of the periciliary fluid layer is approximately 5 to 6 μm (14) while the mucus layer is estimated to be between 5 to 10 μm (15). In the case that the mucus layer is absent, stress will be applied directly to the lower surface of the polymer layer by the cilia. The effect of gravity will be ignored in this analysis. The problem is then reduced to the analysis of the viscoelastic polymer layer with the lower boundary subjected to a time varying velocity signal generated by ciliary action. The upper boundary of the polymer layer, which is exposed to air, can be assumed to be stress free.

To further facilitate and simplify the mathematical analysis, we first consider the polymer layer being composed of a semi-infinite linear viscoelastic medium. Since the propulsive action of the cilia is cyclical in nature, its motion can be represented as a Fourier series sums of harmonic oscillations. Using the superposition principle of linear viscoelastic theory, the resultant velocity profile will be the sum of the fundamental solutions of the velocity profiles due to each individual harmonic oscillation. The solutions obtained from the semi-infinite case are utilized to determine the solution for the finite case by adding up the fundamental solutions that are reflected successively from the two boundaries employing the superposition principle and an assumption on symmetry.

In summary, the mathematical formulation and assumptions of mucociliary flow in the polymer layer can be defined as follow:

a) the polymer layer is first considered to be represented by a semi-infinite linear viscoelastic medium
b) the propulsive action due to the cilia is represented by the boundary condition imposed at the underside surface of the polymer layer
c) the solution for the polymer layer with finite thickness can be determined from the solution of the semi-infinite case by adding the semi-infinite fundamental solutions reflected successively from the boundaries
d) the stress generated by the cilia can be represented as a Fourier series of complex exponential terms and the required solution is obtained by linear superposition of simple solutions
e) the effect of gravity, which may be important at large total depths, has been neglected in this analysis.

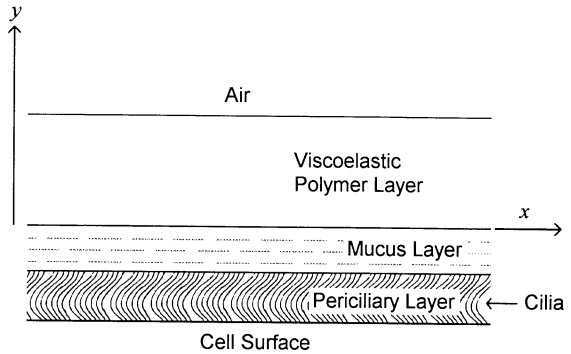

Fig. 1. Schematic illustration of transport of the viscoelastic polymer layer by the mucociliary transport system. Stress generated by cilia is transmitted through the mucus layer to the under side of the viscoelastic polymer layer.

Model Development

First, we consider the polymer layer as composed of a semi-infinite linear viscoelastic medium located in the region $0 \leq y < \infty$. We further assumed that the flow is unidirectional with velocity components as illustrated in figure 2. The underside surface at $y = 0$ is subjected to a sinusoidally varying velocity $v_x(t,0) = V_0 \cdot e^{i\omega t}$ where V_0 is the amplitude of the velocity and ω is the angular frequency.

Following Bird (16), the governing equations for motion in the viscoelastic medium can be described by the equation of continuity:

$$\nabla \cdot \vec{v} = 0, \tag{1}$$

equation of motion:

$$\rho \frac{\partial v_x}{\partial t} = -\frac{\partial}{\partial y} \tau_{yx}, \tag{2}$$

and the constitutive equation:

$$\tau_{yx}(t,y) = -\int_{-\infty}^{t} G(t - t') \frac{\partial v_x(t',y)}{\partial y} dt', \tag{3}$$

where $\vec{v} = (v_x, v_y, v_z)^T$ is the velocity vector and v_x, v_y and v_z are the components of $\vec{v}$ in the x, y and z direction respectively; t is the time; $G(t)$ is the stress relaxation function due to a unit step strain; ρ is the density; τ_{yx} is a second order tensor representing the shear stress in the x-direction on a surface normal to the y-axis and t' is a dummy integration variable.

The initial condition is

$$v_x(0,y) = 0 \qquad \text{for} \qquad t = 0,\ y \geq 0, \tag{4}$$

and the boundary conditions are:

$$v_x \to 0 \qquad \text{for} \qquad y \to \infty, \tag{5}$$

$$v_x(t,0) = V_0 e^{i\omega t} \qquad \text{for} \qquad t \geq 0,\ y = 0. \tag{6}$$

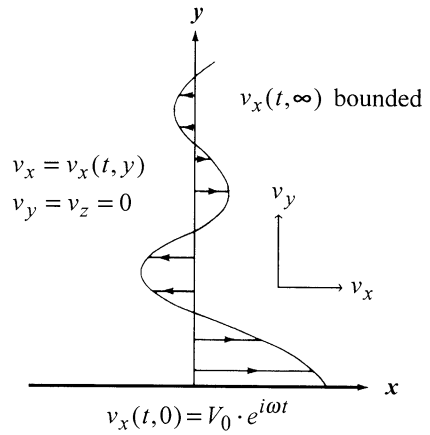

Fig. 2. Idealized model showing the steady state time varying velocity in the viscoelastic polymer layer due to a sinusoidally varying velocity boundary at the polymer mucus interface at $y = 0$.

For uni-directional flow, $v_y = v_z = 0$, the continuity equation is satisfied exactly. Substituting the equation of motion (eq. 2) into the constitutive equation (eq. 3), one obtain

$$\rho \frac{\partial v_x}{\partial t} = \int_{-\infty}^{t} G(t - t') \frac{\partial^2 v_x(t',y)}{\partial y^2} dt'. \quad (7)$$

Since the system is linear, we expect on physical grounds that as $t \to \infty$, the velocity throughout the semi-infinite linear viscoelastic medium will become sinusoidal with the same frequency as the applied velocity signal but exhibiting a phase shift. We can write the long time steady state time varying solution in the following form

$$v_x = V_0 e^{-\alpha y} \cdot e^{i(\omega t - \beta y)}, \quad (8)$$

where α is the attenuation coefficient and β is the phase shift. When this value of v_x is substituted in equation 7, two simultaneous equations in α and β are obtained and ultimately can be used to solve for α and β.

Differentiating v_x from equation 8 with respect to t and y gives

$$\frac{\partial v_x}{\partial t} = i\omega A e^{-(\alpha + i\beta)y} \cdot e^{i\omega t}, \quad (9)$$

$$\frac{\partial v_x}{\partial y} = -(\alpha + i\beta) A e^{-(\alpha + i\beta)y} \cdot e^{i\omega t}, \quad (10)$$

$$\frac{\partial^2 v_x}{\partial y^2} = (\alpha + i\beta)^2 A e^{-(\alpha + i\beta)y} \cdot e^{i\omega t}. \quad (11)$$

Substituting equations 9 and 11 into equation 7, we have

$$\rho i\omega A e^{-(\alpha + i\beta)y} \cdot e^{i\omega t} = \int_{-\infty}^{t} G(t - t') \cdot (\alpha + i\beta)^2 \cdot A e^{-(\alpha + i\beta)y} \cdot e^{i\omega t'} \cdot dt'. \quad (12)$$

Change the variable by substituting $s = t - t'$ into equation 12, one obtain

$$\rho i\omega A e^{-(\alpha + i\beta)y} \cdot e^{i\omega t} = (\alpha + i\beta)^2 \cdot A e^{-(\alpha + i\beta)y} \cdot e^{i\omega t} \cdot \int_0^{\infty} G(s) e^{-i\omega s} \cdot ds. \quad (13)$$

Substituting the definition of complex viscosity, $\eta^* = \int_0^{\infty} G(s) \cdot e^{-i\omega s} \, ds$, into equation 13 and after simplification, equation 13 becomes

$$\rho i\omega = (\alpha + i\beta)^2 \cdot \eta^*, \quad (14)$$

or

$$\frac{\rho i\omega}{\eta^*} = (\alpha + i\beta)^2 . \quad (15)$$

Using the definition of $\eta^* = \eta_1 - i\eta_2$, equation 15 can be written as

$$\frac{\rho i\omega}{\eta_1 - i\eta_2} = (\alpha^2 - \beta^2) + 2\alpha\beta i, \quad (16)$$

where η_1 is the dynamic viscosity and η_2 is the imaginary part of the complex viscosity. Multiplying the left hand side of equation 16 by $(\eta_1 + i\eta_2)/(\eta_1 + i\eta_2)$, we get

$$\frac{\rho\omega\eta_1 i - \rho\omega\eta_2}{(\eta_1^2 + \eta_2^2)} = (\alpha^2 - \beta^2) + 2\alpha\beta i. \quad (17)$$

Consequently, by equating the real and imaginary part of equation 17, we obtain two simultaneous equations in α and β

$$(\alpha^2 - \beta^2) = \frac{-\rho\omega\eta_2}{(\eta_1^2 + \eta_2^2)}, \quad (18)$$

$$2\alpha\beta = \frac{\rho\omega\eta_1}{(\eta_1^2 + \eta_2^2)} . \quad (19)$$

From equations 18 and 19, we can solve for α and β and obtain[4]

$$\alpha = \frac{1}{|\eta^*|} \sqrt{\frac{\rho\omega}{2}(|\eta^*| - \eta_2)}, \quad (20)$$

$$\beta = \frac{\eta_1}{|\eta^*|} \sqrt{\frac{\rho\omega}{2(|\eta^*| - \eta_2)}} . \quad (21)$$

where $|\eta^*| = \sqrt{\eta_1^2 + \eta_2^2}$ is the magnitude of the complex viscosity η^*.

Substituting the definition of storage modulus $G_1 = \omega\eta_2$, loss modulus $G_2 = \omega\eta_1$ and loss tangent $\tan\delta = G_2/G_1$ into equation 20 and after simplification the attenuation coefficient α can be expressed as

$$\alpha = \frac{\omega}{\sqrt{1 + \tan^2\delta}} \sqrt{\frac{\rho}{2G_1}(\sqrt{1 + \tan^2\delta} - 1)}. \quad (22)$$

The fundamental solution (eq. 8) obtained from the semi-infinite case can be extended to the case of a finite viscoelastic medium of thickness l, subjected to an applied oscillatory velocity $v_x(t,0) = V_0 \cdot e^{i\omega t}$ at the underside surface $y = 0$, and with the other end free. This implies that the shear stress at $y = l$ is equal to zero, or equivalently, the velocity gradient $\partial v_x/\partial y = 0$.

Since the viscoelastic medium is linear, solution for the finite thickness case can be obtained by adding successively reflected semi-infinite fundamental solutions from the two boundaries using the superposition principle and symmetry argument. This resulted in the solution for the finite thickness case as[5]

$$v_x = \sum_{n=0}^{\infty} (-1)^n V_0 e^{-\alpha(2nl + y)} \cdot e^{i[\omega t - \beta(2nl + y)]} + \sum_{n=1}^{\infty} (-1)^{n+1} V_0 e^{-\alpha(2nl - y)} \cdot e^{i[\omega t - \beta(2nl - y)]} . \quad (23)$$

[4] The derivation is available from the authors upon request.

[5] The derivation is available from the authors upon request.

MATERIALS AND METHODS

Measurement of Mucociliary Transport

An *in vitro* (also termed *ex vivo*) technique commonly used to study mucociliary transport is the excised frog palate model. The ciliated epithelium of the frog palate has been used frequently as a model for evaluating the role of rheological properties of mucus on mucociliary transport velocity (17,18,19) and has become a classical model for evaluation of mucociliary transport (20). The advantages of the *ex vivo* technique are a) more control over experimental variables; b) easier to perform experiments; and c) less cost. The bullfrog (Rana Catesbiana) palate provides a broad, flat area of mucosa surface for testing the transport rate *in vitro*. The ciliated mucosa of the palate closely resembles that of mammalian respiratory epithelium morphologically, functionally and histochemically (19,21). Furthermore, the frog palate does not need to be maintained within a narrow temperature range to remain viable.

Large bullfrogs (Rana Catesbiana) with a body length of 5–6 inches or longer were purchased from Western Scientific (West Sacramento, CA). The frog was sacrificed by decapitation. The upper palate was dissected free of the body with careful handling to avoid damaging the mucosa. Experiments were performed at controlled room temperature (23–26°C) with the palate completely enclosed in a humidified chamber and with frequent rinsing with frog ringer solution. The frog ringer solution (90 mM NaCl, 3 mM KCl, 2 mM $CaCl_2$ and 15 mM $NaHCO_3$ per liter and pH 7.8) was used to bathe the palate (20). The palate was placed inside the humidified chamber with the palate side facing up. Transport along the palate was observed with a dissecting microscope (Stereo 2, Cambridge Instruments) at a magnification of 20×. Regions of active ciliary motility were determined by the rhythmical flickering of light from the mucosal surface. The parasphenoid (midline of the palate) region or the orbital region near the eustachian tube was used to study the transport rate. The dissecting microscope fitted with a calibrated eye piece micrometer was placed over the line of ciliary transport. The transport can easily be determined by depositing tracer particles (charcoal powder, 100 mesh, 150 μm) on the palate and measuring the time required for traveling a given distance. A baseline transport velocity was determined for endogenous frog mucus (approx. 10 to 15 mm/min.) before each testing of the polymer samples. Transport velocity of the polymer sample was determined by placing a small aliquot (10–15 mg) of the polymer on top of the mucus layer of the palate. The results were normalized by the baseline transport velocity and expressed in terms of relative transport rate (*TR*) corresponding to the ratio of polymer transport velocity to the baseline velocity. The baseline and polymer transport readings were measured within 3 minutes. Measurements were repeated on at least 3 separate palates and results were averaged.

Viscoelastic Measurement of Polymers

The polymers tested for mucociliary transportability on the frog palate were poly(ethylene oxide) with approximate weight average molecular weights of 100K, 600K, 2 and 5 million dalton (Polyox® WSR N-10, WSR-205, WSR N-60K and WSR Coagulant respectively from Union Carbide, Danbury, CT); hydroxylpropyl methylcellulose (HPMC, Methocel® E10M from Dow Chemical, Midland, MI) and 1:1 equivalent triethanolamine (Sigma Chemical, St. Louis, MO) neutralized polyacrylic acid (Carbopol® 934P from B.F. Goodrich, Brecksville, OH). All polymer gels were prepared by thoroughly dispersing an appropriate amount of polymer in water.

The dynamic viscoelastic parameters were measured with the controlled stress RTI Visco-Elastic Rheometer (Krüss, Royston Herts, U.K.) in oscillatory mode using either the cone and plate (CP005) or the coaxial cylinder (CC13) measuring systems. The sample was subjected to a sinusoidal oscillatory shear stress at a preset frequency and the strain response was monitored by the control console. Data collection is via computer interface and the viscoelastic parameters were calculated by computer software developed by Krüss. To ensure that the polymer gels were examined in their linear viscoelastic region, the amplitude sweep at a fixed frequency (0.1 or 1.0 Hz) was first tested to identify the region in which the complex moduli were independent of the stress amplitude. A stress amplitude was then selected in the linear region that would give a strain amplitude of sufficient magnitude above the sensitivity limit of the instrument to ensure a good signal to noise ratio. A thin layer of mineral oil was applied along the edge of the cone and plate or the top of the coaxial measuring system to prevent excessive solvent evaporation. The measurements were performed at 30.0 ± 0.5°C at frequency of 1 Hz. The ratio of the stress vector in phase with the strain vector to the strain defines the storage modulus (G_1) and the ratio of the stress vector 90° out of phase with the strain vector to the strain defines the loss modulus (G_2). For a perfect elastic material, the stress is in phase with the strain. On the other hand, for a perfect viscous material, the stress is 90° out of phase with the strain. Between these two extremes define viscoelastic behavior. The storage modulus (G_1) is indicative of elastic behavior that shows the ability of the polymeric system to store elastic energy associated with recoverable elastic deformation. The loss modulus (G_2) is a measure of the dynamic viscous behavior which relates to the dissipation of energy associated with unrecoverable viscous loss. The loss tangent (tan δ) is defined as the ratio of the loss modulus to the storage modulus (i.e., $\tan \delta = G_2/G_1$) and is dimensionless. It is a measure of the ratio of the energy lost to energy stored in a cycle of deformation, and provides a comparative parameter that combines both the elastic and viscous contributions to the system (22).

RESULTS

The results from the frog palate transport studies are depicted in figures 3 to 5. An apparent negative relationship is observed between the relative transport rate (*TR*) and the storage (G_1) or loss (G_2) modulus, i.e., the transport rate decreases as G_1 or G_2 increases. The relative transport rate decreases in an almost linear fashion on a double log plot. In spite of the wide differences in molecular weights and structures among the polymers tested, the pooled results are

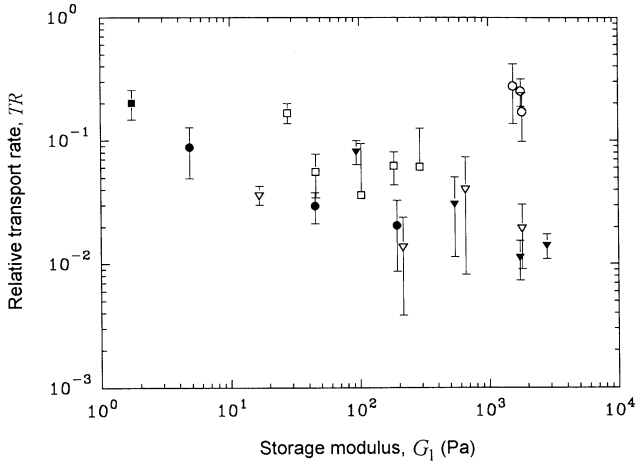

Fig. 3. Relative frog palate transport rate as a function of storage modulus (G_1) for various hydrophilic polymer gels. The storage modulus was determined at 1Hz and 30°C. Key: (■) Polyox 100K MW 20%; (●) Polyox 600K MW 5, 7.5, 10%; (▽) Polyox 2 million MW 2.5, 5, 7.5, 10%; (▼) Polyox 5 million MW 2.5, 5, 7.5, 10%; (□) Methocel E10M (HPMC) 2, 2.5, 3, 3.5, 4%; and (○) Neutralized Carbopol 934P 1, 1.5, 2%.

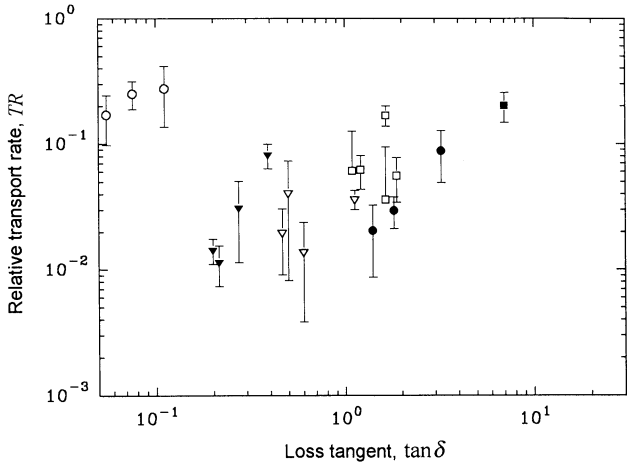

Fig. 5. Relative frog palate transport rate as a function of loss tangent (tan δ) for various hydrophilic polymer gels. The loss tangent was determined at 1Hz and 30°C. Key: (■) Polyox 100K MW 20%; (●) Polyox 600K MW 5, 7.5, 10%; (▽) Polyox 2 million MW 2.5, 5, 7.5, 10%; (▼) Polyox 5 million MW 2.5, 5, 7.5, 10%; (□) Methocel E10M (HPMC) 2, 2.5, 3, 3.5, 4%; and (○) Neutralized Carbopol 934P 1, 1.5, 2%.

found to follow a general trend in terms of mucociliary transportability behavior and polymer viscoelastic characteristics. This is in general agreement with the observation by King (23) and Gelman et al. (24) in that mucociliary transport is a function of the rheological property rather than the chemical properties of the viscoelastic mucus. Furthermore, King et al. (18) have demonstrated that many hydrophilic polymers, which are chemically quite different from mucus, are able to restore transport on a mucus depleted frog palate. Figure 5 shows a double log plot of relative transport rate (*TR*) vs. loss tangent (tan δ). A minimum in *TR* is observed for a tan δ value of about 0.7 to 0.9.

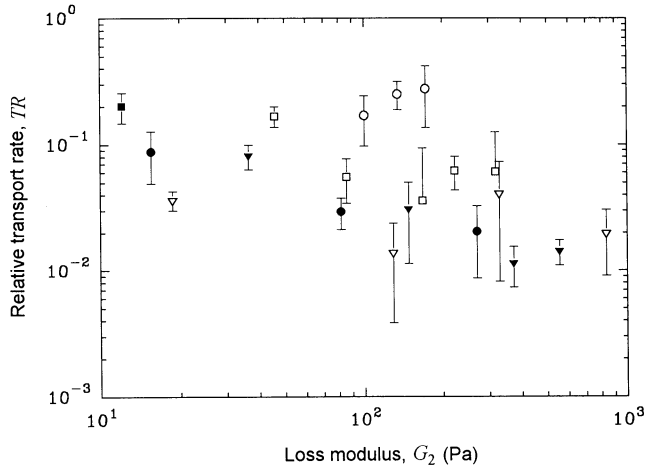

Fig. 4. Relative frog palate transport rate as a function of loss modulus (G_2) for various hydrophilic polymer gels. The loss modulus was determined at 1Hz and 30°C. Key: (■) Polyox 100K MW 20%; (●) Polyox 600K MW 5, 7.5, 10%; (▽) Polyox 2 million MW 2.5, 5, 7.5, 10%; (▼) Polyox 5 million MW 2.5, 5, 7.5, 10%; (□) Methocel E10M (HPMC) 2, 2.5, 3, 3.5, 4%; and (○) Neutralized Carbopol 934P 1, 1.5, 2%.

Comparison of Computed Model Values with Experimental Data

The force generated by cilia is relatively constant and has been estimated to be about 4×10^{-7} dynes per cilium (14). For a given force, the extent of deformation in the viscoelastic medium decreases as the magnitude of the modulus increases. This implies that mucociliary transport decreases with a decreasing degree of deformability of the viscoelastic medium. Therefore, the frog palate relative mucociliary transport rate (*TR*) must be adjusted to account for the differences in moduli. The moduli adjusted transport rate ($TR_{|G^*|}$) is defined as

$$TR_{|G^*|} = |G^*| \cdot TR, \tag{24}$$

where $|G^*| = \sqrt{G_1^2 + G_2^2}$ is the magnitude of the complex modulus.

From equation 23, we see that the velocity, v_x, in the viscoelastic medium at a given time is a function of the attenuation coefficient α and the distance y. For a given y, the velocity, v_x, decreases with increasing α. Therefore, to a first approximation, we expect the moduli adjusted relative transport rate ($TR_{|G^*|}$) to be inversely proportional to the attenuation coefficient α. That is,

$$(TR_{|G^*|})^{-1} = k\alpha = k \frac{\omega}{\sqrt{1 + tan^2\,\delta}} \sqrt{\frac{\rho}{2G_1}} \sqrt{1 + \tan^2\delta - 1}\,, \tag{25}$$

where k is the proportionality constant.

Substituting $|G^*| = \sqrt{G_1^2 + G_2^2}$ and $TR_{|G^*|} = |G^*| \cdot TR$ into equation 25 and after simplification, one obtain

$$TR^{-1} = k' \sqrt{G_1} \left[\sqrt{\sqrt{1 + \tan^2\delta} - 1} \right] \tag{26}$$

where $k' = k\omega\sqrt{\rho/2}$.

Taking the logarithm of both sides of equation 26, after rearrangement the resulting equation is

$$\log(TR_{\tan\delta}) = -\frac{1}{2}\log(G_1) + \log\frac{1}{k'} \qquad (27)$$

where $TR_{\tan\delta} = TR \cdot [\sqrt{\sqrt{+\tan^2\delta} - 1}]$ is the *"loss tangent adjusted transport rate."* Since mucociliary transport depends on two independent fundamental viscoelastic parameters, the adjustment is necessary in order to isolate the dependence of transport rate only on one single viscoelastic parameter.

From equation 27, we see that at a fixed angular frequency ω, $\log(1/k')$ is constant and a plot of $\log(TR_{\tan\delta})$ vs. $\log(G_1)$ would yield a straight line with slope and y-intercept equal to $-1/2$ and $\log(1/k')$ respectively. The double log plot of relative transport rate adjusted for primary variations due to $\tan\delta$ ($TR_{\tan\delta}$) against the storage modulus (G_1) is depicted in figure 6. The slope of the linear regression line on the $\log(TR_{\tan\delta})$ vs. $\log(G_1)$ plot is equal to -0.571, which is very close to the theoretical value of -0.5; while the y-intercept, $\log(1/k')$, and r^2 are equal to -0.3842 and 0.7142 respectively.

Rearranging equation 25 results in

$$TR_{G_1} = \frac{1}{k'} f(\tan\delta), \qquad (28)$$

where $f(\tan\delta) = [(1/(1 + \tan^2\delta))\sqrt{\sqrt{1 + \tan^2\delta} - 1}]^{-1}$ and $TR_{G_1} = (|G^*| \cdot TR)/(\sqrt{G_1})$ is the *"storage modulus adjusted transport rate."*

Therefore a plot of TR_{G_1} vs. $\tan\delta$ is expected to follow the same functional dependency as $f(\tan\delta)$ to $\tan\delta$. The double log plot of TR_{G_1} and $f(\tan\delta)/k'$ vs. $\tan\delta$ is depicted in figure 7.

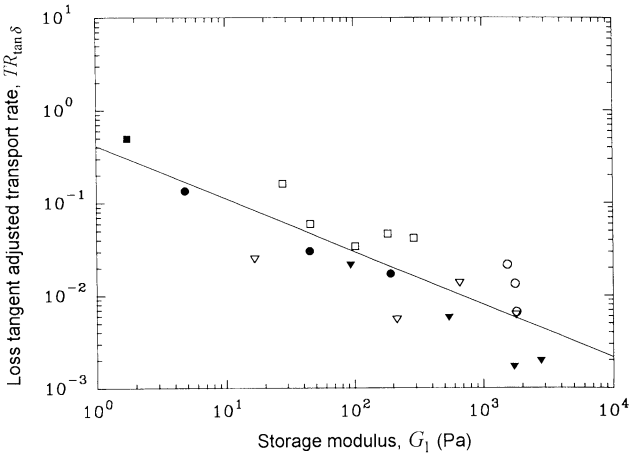

Fig. 6. Double log plot of loss tangent adjusted transport rate ($TR_{\tan\delta}$) vs. storage modulus (G_1) for various hydrophilic polymer gels. The storage modulus was determined as 1Hz and 30°C. Key: (□) Polyox 100K MW 20%; (■) Polyox 600K MW 5, 7.5, 10%; (●) Polyox 2 million MW 2.5, 5, 7.5, 10%; (▽) Polyox 5 million MW 2.5, 5, 7.5, 10%; (▼) Methocel E10M (HPMC) 2, 2.5, 3, 3.5, 4%; and (○) Neutralized Carbopol 934P 1, 1.5, 2%.

DISCUSSION

A theoretical model would be of little use if it does not conform to experimental data. Theoretical and experimental results are compared in figures 6 and 7, and to a first approximation, there is general agreement between theory and experiment. In this model, we propose as a first approximation, that the moduli adjusted transport rate, $TR_{|G^*|}$, is inversely proportional to the attenuation coefficient, α. The approximation simplifies the mathematical treatment of the model, but it is important to recognize the limitation of this approximation approach. This is especially true at the two extreme cases where the loss tangent is equal to zero and to infinity. A loss tangent equal to zero implies that the loss modulus (G_2) is also equal to zero. In this case, there is no dissipative loss and the medium behaves perfectly elastic. The attenuation coefficient α is identically zero in this case. On the contrary, when the loss tangent approaches infinity, the storage modulus (G_1) approaches zero. The medium then behaves as purely viscous. In this case, the equation of motion, together with the constitutive equation for a Newtonian fluid degenerates to the Navier-Stokes equation. We did not pursue the two extreme cases in this analysis.

From equation 28, it is possible to deduce the optimal rheological properties that a polymeric formulation must possess in order to minimize its clearance by the mucociliary transport system. First, we want to minimize the function, $f(\tan\delta)$. It can be shown that the minimum for $f(\tan\delta)$ occurs at $\tan\delta$ equal to 1.74. Since $\tan\delta$ is equal to the ratio of loss modulus to storage modulus (G_2/G_1), therefore, once the value of $\tan\delta$ is fixed, G_1 is proportional to G_2. The value of $\tan\delta$ depends on polymer structure, molecular weight, degree of cross linking, inter and intra molecular interactions as well as the concentration of the polymer. Secondly, it is also desirable to have the magnitude of the complex modulus, $|G^*|$, as large as possible. This can usually be achieved by increasing the concentration of the polymer.

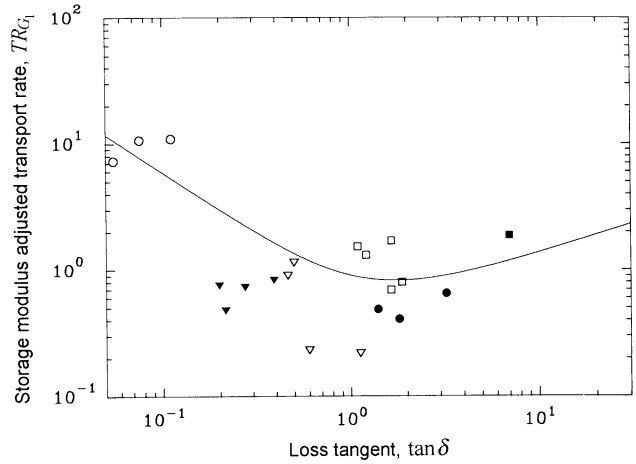

Fig. 7. Double log plot of storage modulus adjusted transport rate (TR_{G_1}) vs. loss tangent (tan δ) for various hydrophilic polymer gels. The loss tangent was determined at 1Hz and 30°C. Key: (□) Polyox 100K MW 20%; (■) Polyox 600K MW 5, 7.5, 10%; (●) Polyox million MW 2.5, 5, 7.5, 10%; (▽) Polyox 5 million MW 2.5, 5, 7 10%; (▼) Methocel E10M (HPMC) 2, 2.5, 3, 3.5, 4%; and (○) N tralized Carbopol 934P 1, 1.5, 2%.

ACKNOWLEDGMENTS

This work was supported in part by Rugby-Darby Group Companies, Inc. and the American Foundation for Pharmaceutical Education.

REFERENCES

1. L. Illum. The nasal delivery of peptides and proteins. *Trends in Biotechnology* **9**:284–289 (1991).
2. Y. W. Chien and S. F. Chang. *Transnasal Systemic Medications,* Elsevier, Amsterdam, 1985.
3. Y. W. Chien, S. E. Su and S. F. Chang. *Nasal Systemic Drug Delivery,* Marcel Dekker, New York, 1989.
4. A. M. Lucas and L. C. Douglas. Principles underlying ciliary activity in the respiratory tract II. A comparison of nasal clearance in man, monkey and other mammals. *Arch. Otolaryng.* **20**:518–541 (1934).
5. Y. Roth, E. F. Aharonson, H. Teichtahl., G. L. Baum, Z. Priel and M. Modan. Human in vitro nasal and tracheal ciliary beat frequencies: comparison of sample sites, combined effect of medication, and demographic relationships. *Ann. Otol. Rhinol. Laryngol.* **100**:378–384 (1991).
6. A. Wanner. Clinical aspects of mucociliary transport. *Am. Rev. Resp. Dis.* **116**:73–125 (1977).
7. M. J. Sanderson and M. A. Sleigh. Ciliary activity of cultured rabbit tracheal epithelium: beat pattern and metachrony. *J. Cell Sci.* **47**:331–347 (1981).
8. M. A. Sleigh. The nature and action of respiratory tract cilia. In J. D. Brian, D. F. Proctor and L. M. Reid (eds.), *Respiratory Defense Mechanism Part I,* Marcel Dekker, New York, 1977, pp. 247–288.
9. M. Litt. Mucus rheology and mucociliary clearance. *Mod. Probl. Paediat.* **19**:175–181 (1977).
10. T. Deitmer. Physiology and pathology of the mucociliary system. Special regards to mucociliary transport in malignant lesions of the human larynx. *Advances in Oto-Rhino-Laryngology* **43**:1–136 (1989).
11. J. S. Chu, R. Chandrasekharan, G. L. Amidon, N. D. Weiner and A. H. Goldberg. Viscometric study of polyacrylic acid systems as mucoadhesive sustained-release gels. *Pharm. Res.* **8(11)**:1408–1412 (1991).
12. J. R. Blake and M. A. Sleigh. Mechanics of ciliary locomotion. *Biol. Rev.* **49**:85–125 (1974).
13. J. R. Blake and H. Winet. On the mechanics of muco-ciliary transport. *Biorheology* **17**:125–134 (1980).
14. A. Silberberg. Biorheological matching: mucociliary interaction and epithelial clearance. *Biorheology* **20**:215–222 (1983).
15. M. A. Sleigh, J. R. Blake and N. Liron. The propulsion of mucus by cilia. *Am. Rev. Resp. Dis.* **137**:726–741 (1988).
16. R. B. Bird, R. C. Armstrong and O. Hassager. *Dynamics of Polymeric Liquids* Vol. I, John Wiley and Sons, New York, 1987.
17. T. M. Chen and M. J. Dulfano. Mucus viscoelasticity and mucociliary transport rate. *J. Lab. Clin. Med.* **91(3)**:423–431 (1978).
18. M. King, A. Gilboa, F. A. Meyer and A. Silberberg. On the transport of mucus and its rheological simulants in ciliated system. *Am. Rev. Resp. Dis.* **110**:740–745 (1974).
19. J. Sade, N. Eliezer, A. Silberberg and A. C. Nevo. The role of mucus in transport by cilia. *Am. Rev. Resp. Dis.* **102**:48–52 (1970).
20. B. K. Rubin, O. Ramirez and M. King. Mucus depleted frog palate as a model for study of mucociliary clearance. *J. Appl. Physiol.* **69(2)**:424–429 (1990).
21. M. J. Dulfano and K. B. Adler. Physical properties of sputum VII. Rheologic properties and mucociliary transport. *Am. Rev. Resp. Dis.* **112**:341–347 (1975).
22. J. D. Ferry. *Viscoelastic Properties of Polymers,* John Wiley and Sons, New York, 1980.
23. M. King. Relationship between mucus viscoelasticity and ciliary transport in guaran gel/frog palate model system. *Biorheology* **17**:249–254 (1980).
24. R. A. Gelman and F. A. Meyer. Mucociliary transference rate and mucus viscoelasticity. Dependence on dynamic storage and loss modulus. *Am. Rev. Resp. Dis.* **120**:553–557 (1979).